

ECMWF Feature article

.....
from Newsletter Number 147 – Spring 2016

METEOROLOGY

.....
New model cycle brings
higher resolution
.....



Based on an image from mirgao/iStock/Thinkstock

www.ecmwf.int/en/about/news-centre/media-resources

doi:10.21957/s2gvuwmg

This article appeared in the Meteorology section of ECMWF Newsletter No. 147 – Spring 2016, pp. 14–19.

New model cycle brings higher resolution

Elías Hólm, Richard Forbes, Simon Lang, Linus Magnusson, Sylvie Malardel

On 8 March 2016, ECMWF introduced a new model cycle of the Integrated Forecasting System (IFS) into operations. Cycle 41r2 represents a significant step forward in accuracy and resolution and, at a grid spacing of 9 km, it is currently the highest-resolution global forecasting system in the world. The main change is an increase in horizontal resolution in most parts of the forecasting system. For high-resolution forecasts (HRES) and ensemble forecasts (ENS) the grid-point resolution is roughly doubled to 9 km and 18 km, respectively, while for the Ensemble of Data Assimilations (EDA) it is tripled to 18 km. In combination with several other scientific and technical changes, this has led to a significant increase in forecast accuracy and computational efficiency. This article sets out the main changes leading to improvements in forecast quality.

Resolution increase and new grid

The 2016 horizontal resolution upgrade is designed to achieve a balance between greater resolution and increased forecast accuracy on the one hand and computational cost on the other. A number of combinations of horizontal resolutions were tried for 4DVAR, EDA, HRES and ENS. The solution that was eventually adopted is summarised in Table 1.

The main innovation in the resolution upgrade is the introduction of a new ‘cubic octahedral’ grid (with new prefix ‘O’ to distinguish it from the reduced Gaussian grid with prefix ‘N’). The cubic octahedral grid is based on a cubic spectral truncation and a new mesh that allows for the future implementation of a hybrid spectral/grid-point model. The new grid is described in detail in *Malardel et al. (2016)*. The change from the current linear (TL) to a cubic (TC) spectral truncation means that the shortest resolved wave is represented by four rather than two grid points. This change was made because in the IFS a cubic grid leads to more accurate forecasts than a linear grid at the same computational cost. The cubic octahedral grid, denoted by TCo, increases the resolution in grid-point space somewhat less and is 25% less costly than a TC grid at the same spectral truncation.

Average grid spacing	HRES	ENS		4DVAR inner loops			EDA		
		Medium-range	Monthly extension	1st	2nd	3rd	Outer	1st	2nd
128 km								TL159	TL159
				TL255	TL255	TL255		TL191	TL191
64 km			TL319		TL319				
						TL399			
32 km		TL639	TCo319					TL399	
									TCo639
16 km	TL1279	TCo639							
9 km	TCo1279								

Table 1 The new model cycle brings a number of resolution upgrades across the forecasting system. The table shows the changes from Cycle 41r1 (blue) to Cycle 41r2 (red). TL stands for triangular-linear and TCo for triangular-cubic-octahedral. The numbers indicate the spectral truncation.

The benefits of the cubic grid can be seen in increased realism at smaller scales, where less diffusion is needed than for a linear grid, and where there is no need for a dealiasing filter because now four points represent the shortest wave. The efficiency of representation of the kinetic energy spectrum (Figure 1) is significantly improved, with more energy in the smaller scales due to a reduction of the diffusion and the removal of the dealiasing filter. There is also consistency between the analysis and forecast spectra, which was not the case with the linear grid, where the analysis trajectory required stronger diffusion than the forecast.

The improved consistency between analyses and forecasts in 41r2 can be seen in Figure 2, where the level of detail in 2-metre temperature is very similar in the 41r2 analysis and forecast, whereas the analysis in 41r1 is smoother than the 41r1 forecast. The increased level of small-scale detail going from 41r1 to 41r2 is also visible.

In general the increased resolution leads to a better representation of coastlines and orography with consistent gains in forecast performance in the tropics and extra-tropics for 2-metre temperature, 2-metre humidity, and 10-metre wind speed. There is also a substantial reduction in localised (unrealistic) precipitation extremes over orography. This is achieved by the cubic grid representation and modifications in the semi-Lagrangian advection scheme, as described by *Malardel et al. (2016)*.

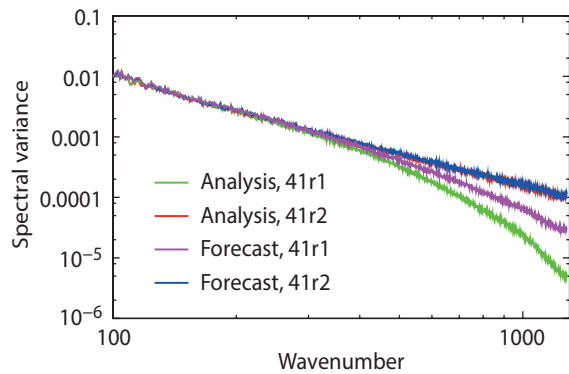


Figure 1 Spectra of kinetic energy at model level 137, the level closest to the surface, shown for HRES analyses and 24-hour forecasts.

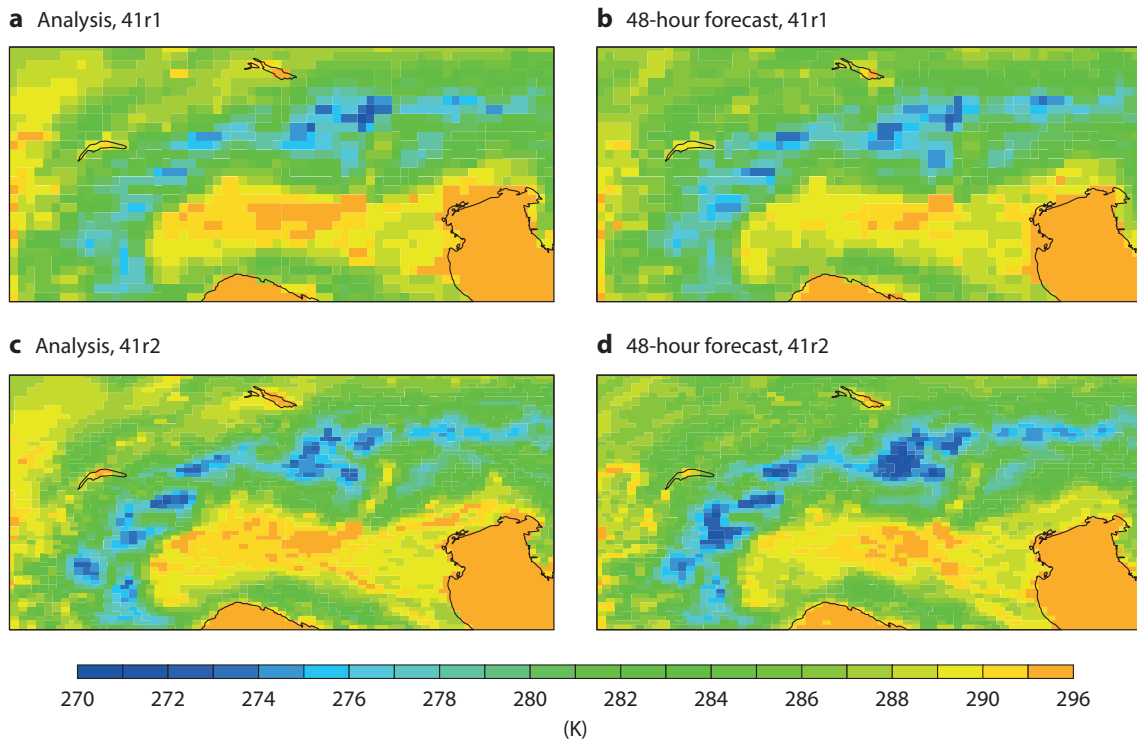


Figure 2 Two-metre temperature valid on 1 June 2015 00 UTC for (a) 41r1 analysis, (b) 41r1 HRES 48-hour forecast, (c) 41r2 analysis and (d) 41r2 HRES 48-hour forecast.

Data assimilation and ensemble forecasts

There are several further improvements in consistency within and between the different forecasts and analyses. Increasing the ensemble forecast and EDA resolution to TCo639, which is 18 km in grid-point space, brings both close to the 16 km resolution of the previous high-resolution forecast. In addition to improved overall ensemble forecast scores, the higher resolution also leads to improved analyses and forecasts of tropical cyclones. The tracks and in particular the intensity of tropical cyclones are now more accurate due to the increased resolution, which enables more accurate modelling of smaller and deeper tropical cyclones. This can be seen in Figure 3, which shows that forecasts of the core pressure of tropical cyclones have become more accurate (smaller root-mean-square error) while the spread has increased, which improves the forecast reliability.

The resolution increase of the analysis increments of 4DVAR ('inner loops') to TL399 is the second main factor – after the forecast resolution increase – responsible for the overall improvement in forecast skill. The combination of higher-resolution forecasts and inner loops results in a closer fit between measurements and the model, which enables a better use of space-based and in-situ high-resolution observations. The increased resolution of the analysis increments also enables corrections at smaller scales. For Cycle 41r2, most of the systematic tests of different inner-loop options used linear grids. The best compromise between computational cost and forecast accuracy was achieved by a 4DVAR with three inner loops with resolution TL255 followed by TL319 and TL399. Cubic-octahedral inner loops will be considered for later cycles.

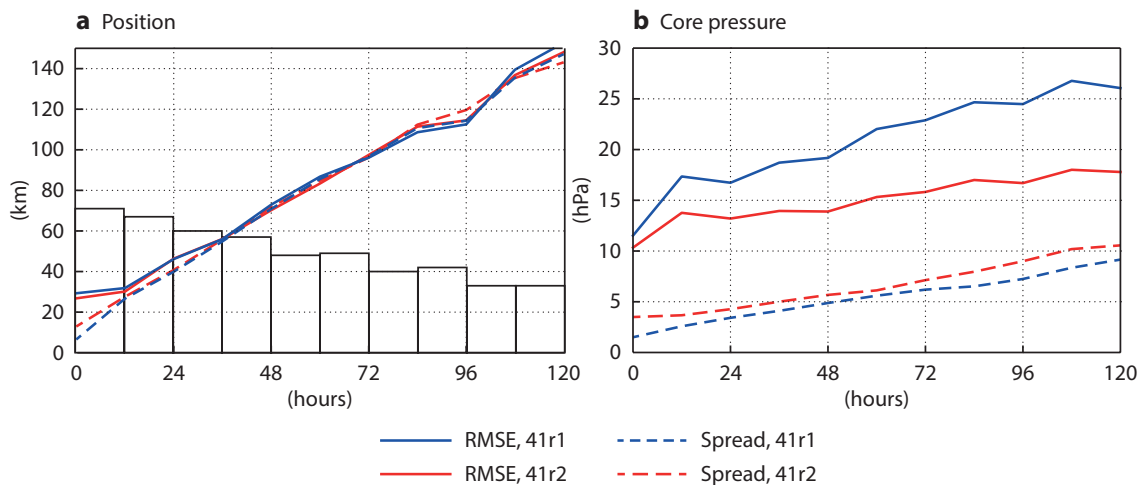


Figure 3 Root-mean-square error (RMSE) and spread of ensemble forecasts of tropical cyclone track and intensity for 45 initial dates in total from June to July 2015, showing (a) position error and spread and (b) core pressure error and spread. The sample size, indicated by the bars in (a), starts from 70 at 0 hours and reduces gradually to half that number at 120 hours.

The improvement in ensemble forecasts depends on the complex interaction between ENS, EDA and HRES, because the ENS initial state includes improved EDA forecasts centred on improved HRES analyses. This can be illustrated by looking at a typical tropical cyclone case, Ula in Figure 4, which shows 10-day ensemble and high-resolution forecasts from before (41r1) and after (41r2) the resolution increase. As in the averages in Figure 3, the ensemble members are now closer to observations, with a larger fraction of category HR1 cyclone forecasts, while at the same time the ensemble spread is larger. Another improvement in this case is that the high-resolution forecasts mostly fall within the spread of the ensemble, because on the one hand the spread has become a better estimate of the error (Figure 3) and on the other both HRES and ENS have become more accurate and thus closer to each other. At the start of the forecast, the spread is also larger due to the higher EDA resolution. The improvements in the EDA error and spread are even greater than for other parts of the system because the EDA grid-point resolution has more than tripled.

The consistency in ENS was also improved by moving the step-decrease in resolution of the forecast (going from 'medium-range' at TCo639 to 'monthly extension' at TCo319) from day 10 out to day 15, thus ensuring consistent high forecast resolutions throughout the medium range to 15 days. This can be seen in the 2-metre temperature Continuous Ranked Probability Score (CRPS) in Figure 5, where in addition to the improved scores for Cycle 41r2, the jump to less accurate forecasts at day 10 seen in Cycle 41r1 is moved to day 15, where it affects forecast accuracy less because the errors at day 15 are larger.

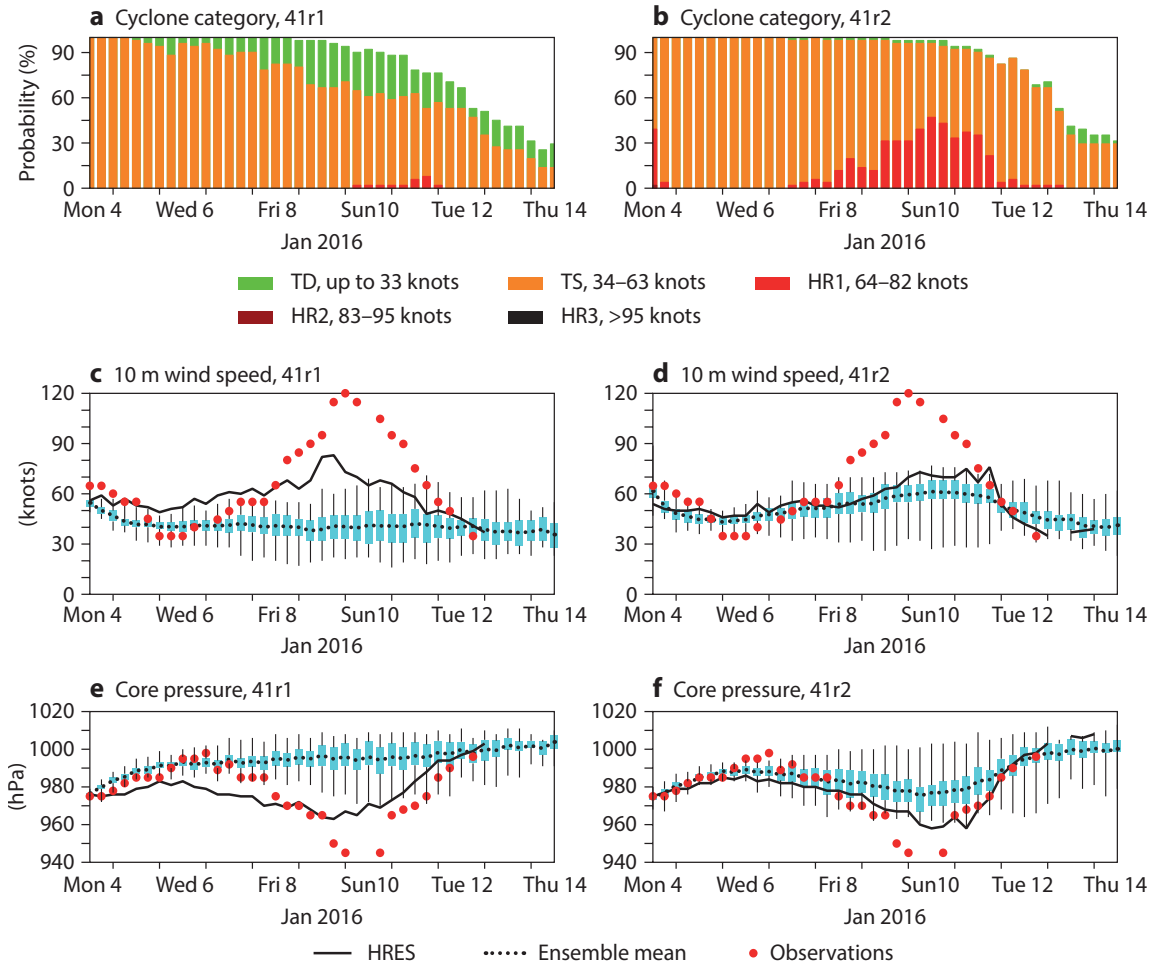


Figure 4 Forecasts for tropical cyclone Ula showing the ENS probability of Ula falling into different strength categories for (a) Cycle 41r1 and (b) Cycle 41r2; ENS and HRES 10-metre wind speed for (c) Cycle 41r1 and (d) Cycle 41r2; and ENS and HRES mean sea level pressure in the cyclone centre with observations for (e) Cycle 41r1 and (f) Cycle 41r2.

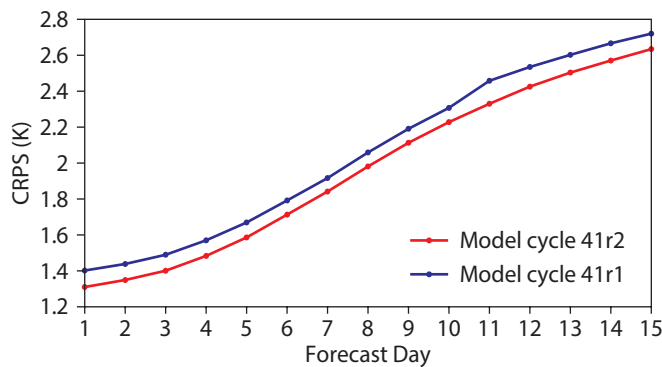


Figure 5 Continuous Ranked Probability Score (CRPS) for ensemble forecasts of 2-metre temperature in Europe averaged over 12 UTC forecasts from 10 August 2015 to 25 February 2016.

Other selected changes

While most of the average improvements in scores come from the increases in resolution – in particular in the forecast resolution and the 4DVAR inner-loop resolution – several other changes to the model have reduced specific systematic forecast errors.

The stability of the semi-Lagrangian numerical scheme near strong wind gradients has been improved, reducing noise downstream of significant orography and in tropical cyclones, and leading to significantly better upper-air forecasts over East Asia, as seen in the lee of the Himalayas in Figure 6 (Diamantakis & Magnusson, 2015).

The modelling of radiative heating/cooling at the surface has been improved by introducing approximate updates on the full grid at every time step. This has led to a reduction in 2-metre temperature errors (Figure 5), particularly near coastlines in places where surface conditions vary abruptly, as described in greater detail by Hogan & Bozzo (2015).

The use of satellite data has also been improved, which has led to improvements in specific areas. For example, microwave data is used in more challenging situations, such as mountain areas and snow-covered land surfaces, and coverage of satellite-derived winds is improved in the mid-latitudes.

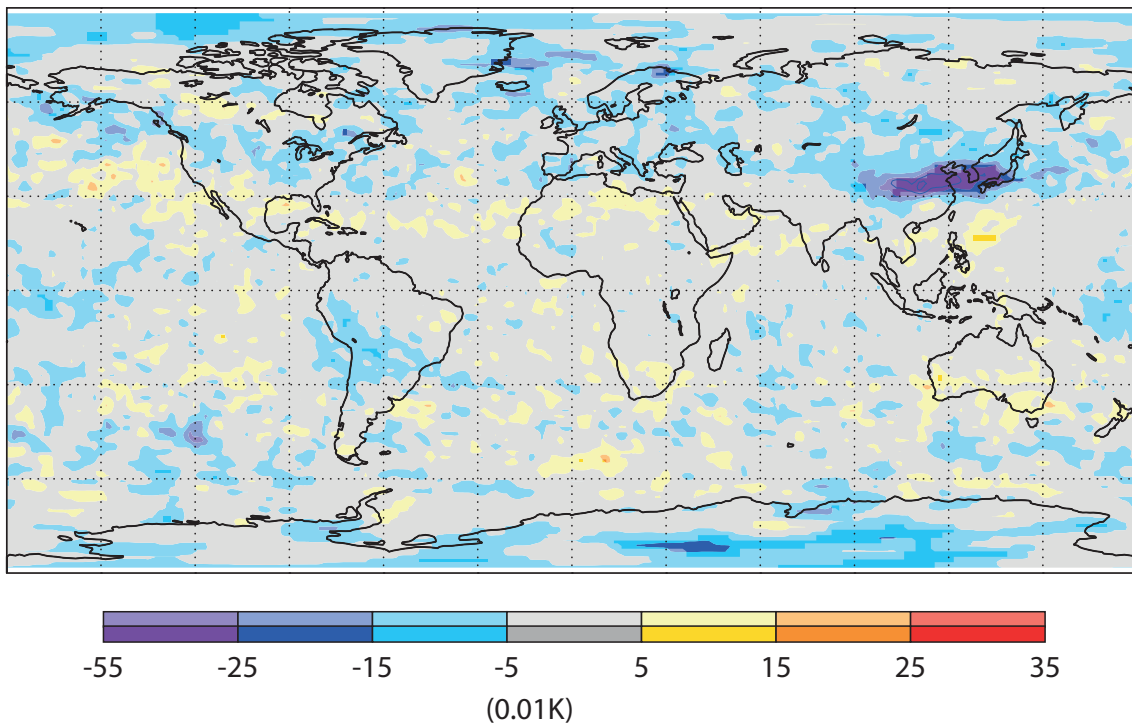


Figure 6 Reduction of 200 hPa temperature day 2 RMSE in HRES forecasts for December/January/February 2015–16 resulting from changes to the semi-Lagrangian advection scheme. Saturated colours denote a significance level of 5%.

Overall improvements

An overview of scores for high-resolution and ensemble forecasts is shown in Figure 7. The performance of both HRES and ENS is improved throughout the troposphere. Error reductions in the order of 2–3% (root-mean-square error and CRPS, respectively) are found for most upper-air parameters and levels. This corresponds to an increase of about 2 hours in the lead time at which the primary headline score for HRES – the 500 hPa geopotential anomaly correlation – drops below 80%. There is an even larger lead time gain for some near-surface parameters, such as a gain of more than 12 hours in ensemble forecasts for 2-metre temperature over Europe, as shown in Figure 5. This is mostly the result of a local reduction in errors in coastal areas with a large land–sea contrast.

Improvements are seen in verification both against the model analysis and against observations. In the tropics, evaluation against model analysis shows an apparent degradation in the short and near-medium range, mostly due to a more active analysis resulting from the increase in resolution of the EDA. Verification against observations, however, gives neutral to positive results in the tropics, except for temperature at 500 hPa and above, which shows a slight degradation. Further improvements to the EDA background error calculation are expected to resolve this in the next operational cycle. There is a small (0.2 K) mean cooling in upper troposphere forecasts. This shows up as an increased root-mean-square error (RMSE) for geopotential at 100 hPa because the mean geopotential in the lower stratosphere is sensitive to changes in the vertically integrated tropospheric temperature. The increased variability of the higher-resolution model also shows up as an apparent degradation in some parameters, for example in waves and precipitation in the tropics.

Summary

Cycle 41r2 has improved the accuracy and consistency of the different components of the IFS, leading to error reductions of 2–3% in tropospheric forecasts. The increase in resolution of the EDA and ENS to 18 km has led to increased realism in the representation of smaller-scale features, such as tropical cyclones, and increased consistency with HRES, which is now the highest-resolution global forecasting system in the world. Several long-standing systematic errors have been reduced through improvements in the model and better use of satellite data, in particular in coastal areas. All these improvements in forecast skill will help forecasters, who will benefit even more once their systems have been adapted to take advantage of the higher-resolution fields.

The work towards IFS Cycle 41r2 achieved a good balance between higher resolution, increased forecast accuracy and affordable computational cost. This was made possible only through intense collaboration involving all parts of ECMWF, including upgrades and optimizations to computing capabilities and supporting software as well as the IFS, together with extensive testing and evaluation.

Further reading

Diamantakis, M. & L. Magnusson, 2015: Numerical sensitivity of the ECMWF model to Semi-Lagrangian departure point iterations. ECMWF Research Department *Technical Memorandum No. 768*.

Hogan, R. & A. Bozzo, 2015: Reducing surface temperature errors at coastlines. *ECMWF Newsletter No. 145*, 30–34.

Hólm, E., M. Bonavita & L. Magnusson, 2015: Improved spread and accuracy in higher-resolution Ensemble of Data Assimilations. *ECMWF Newsletter No. 145*, 15.

Malardel, S., N. Wedi, W. Deconinck, M. Diamantakis, C. Kühnlein, G. Mozdzyński, M. Hamrud & P. Smolarkiewicz, 2016: A new grid for the IFS. *ECMWF Newsletter No. 146*, 23–28.

Siemen, S., I. Russell, T. Quintino & D. Varela Santoalla, 2016: Software updates in preparation for model cycle 41r2. *ECMWF Newsletter No. 146*, 16.

© Copyright 2016

European Centre for Medium-Range Weather Forecasts, Shinfield Park, Reading, RG2 9AX, England

The content of this Newsletter article is available for use under a Creative Commons Attribution-Non-Commercial-No-Derivatives-4.0-Unported Licence. See the terms at <https://creativecommons.org/licenses/by-nc-nd/4.0/>.

The information within this publication is given in good faith and considered to be true, but ECMWF accepts no liability for error or omission or for loss or damage arising from its use.